Proceedings of the 17th World Congress
The International Federation of Automatic Control
Seoul, Korea, July 6-11, 2008

GIMC-based Fault Detection and Its Application to Magnetic Suspension System

Yujiro Nakaso * **Toru Namerikawa** *

* *Division of Electrical Engineering and Computer Science, Kanazawa University, Kakuma-machi Kanazawa, 920-1192, JAPAN*
e-mail: yuji@scl.ec.t.kanazawa-u.ac.jp and toru@t.kanazawa-u.ac.jp

Abstract: This paper deals with a fault detection for a magnetic suspension system by using Generalized Internal Model Control (GIMC) structure. To design robust fault detection filters, two fault detection design problems are formulated as multiple objective optimization problems by minimizing the effects of disturbances and maximizing the fault sensitivity involving an LTI system with disturbance and fault signals. The fault detection filters designed by solving each optimization problems are implemented with the magnetic suspension system to verify its validity. A filter designed via the problem 1 has good transient performance, but the output signal of the filter is affected by the disturbance signals. Another filter which is designed via the problem 2, however, has good robustness for disturbance signals. Moreover, experimental results show that both filters have enough fault detection properties compared with a conventional detection filter.

1. INTRODUCTION

Recently, system management and supervision are needed with very higher quality because the system is to be more complicated and large scale. Therefore, to improve the safety and reliability is necessary for the system which has changed properties and/or had fault. There is one approach for this demand, that is the control system based on GIMC structure. It is high performance for the nominal plant, and reconfigurable to high robustness controller in GIMC structure, Zhou [2001, 2004]. In the literature Namerikawa [2006], GIMC structure is applied to the magnetic suspension system, and experiments are carried out with artificial model perturbation. The validity of the reconfigurability of the GIMC structure is verified because the controller is reconfigured for the corresponding situation of the plant experimentally.

On the other hand, causes of the system perturbation are not only unmodelled dynamics and parameter error, but also failures of the motor or amplifier and positioning error of measuring device. In the worst case, it is posible situation that some actuators and/or some sensors are completely breaking down. When actuator and/or sensor faults are occurred, the performance is degradated or the system is destabilized. Consequently, the fault tolerant control system is required and is very important, which has high performance for the nominal plant, detectability when the plant has some faults, and reconfigurability of the controller to maintain the stability of the system. There are many researches about the fault tolerant control system, Patton [1997], Zhang [2003], Campos-Delgado [2003], Niemann [2005], Liu [2007].

In the fault tolerant control, the fault detection is the first step in the control process, and reconfiguring of the controller is the next step. Therefore the fault detection is very important action in the fault tolerant control. In the literature Liu [2007], the fault detection signal is obtained by a filter for the estimation error signal derived from the GIMC structure for an LTI system including disturbance and fault signals. Since the estimation error signal depends on both signals, disturbance and fault signals, the effect of disturbance should be zero and the effect of fault signals should be dominant. This description is formulated in Liu [2007] as the maximization problem of the fault effection level and optimal fault detection filters are introduced.

In this paper, minimization problems of the disturbance effection level are formulated for the fault detection filter, the optimal solutions are introduced. Calculated filters are implemented with an unstable system, the magnetic suspension system. Furthermore, controllers are designed for the nominal plant and the faulty plant to construct the GIMC structure. It is verified that designed fault detection filters are valid for the fault tolerant control system experimentally. Finally, designed fault detection filters are compared and it is shown that one filter has better performance for disturbance attenuation.

2. NOTATIONS

In this section, we will show definitions of the norm. $\bar{\sigma}$ and $\underline{\sigma}$ represent the maximum singular value and the minimum singular value, respectively. Let $G^*(s) := G^T(-s)$ be the para-Hermitian complex conjugate transpose of $G(s)$.

For $G \in \mathcal{R}H_2$ we define the H_2 norm of G as follows.

$$\|G\|_2 = \sqrt{\frac{1}{2\pi}\int_{-\infty}^{\infty} \mathrm{Trace}\Big\{G^*(j\omega)G(j\omega)\Big\}d\omega} \qquad (1)$$

For $G \in \mathcal{R}H_\infty$ we define the H_∞ norm of G as

$$\|G\|_\infty = \sup_{\omega\in\mathbb{R}} \bar{\sigma}(G(j\omega)), \tag{2}$$

and the H_- norm over all frequency is defined as

$$\|G\|_- = \inf_{\omega\in\mathbb{R}} \underline{\sigma}(G(j\omega)) \tag{3}$$

where $\underline{\sigma}(\cdot)$ is smallest nonzero singular value.

The H_- norm of G over frequency range $[f_1, f_2]$ is defined as follows.

$$\|G\|_-^{[f_1,f_2]} = \inf_{\omega\in[\omega_1,\omega_2]} \underline{\sigma}(G(j\omega)) \tag{4}$$

where $\omega_i = 2\pi f_i$.

3. PROBLEM FORMULATION

Consider an LTI system as follows.

$$\begin{cases} \dot{x} = Ax + B_u u + B_d d + B_f f \\ y = Cx + D_u u + D_d d + D_f f \end{cases} \tag{5}$$

where the state vector $x \in \mathbb{R}^n$, the control input vector $u \in \mathbb{R}^{n_u}$, the disturbance vector $d \in \mathbb{R}^{n_d}$, the fault vector $f \in \mathbb{R}^{n_f}$ and the output vector $y \in \mathbb{R}^{n_y}$. Then the system equation with Laplace transform of these equations is given by

$$y(s) = G_u(s)u(s) + G_d(s)d(s) + G_f(s)f(s) \tag{6}$$

$$[\, G_u \; G_d \; G_f \,] = \left[\begin{array}{c|ccc} A & B_u & B_d & B_f \\ \hline C & D_u & D_d & D_f \end{array}\right]. \tag{7}$$

The following assumptions will be made throughout the paper.

***Assumption** 1.* (A, C) is detectable.

***Assumption** 2.* D_f has full row rank.

***Assumption** 3.* The transfer matrix G_f has no transmission zero on the j-axis.

Assumption 1 ensures that the model can be represented in left coprime factorization. Assumption 2 and 3 are required for technical reasons in spectral factorization.

Since G_u, G_d and G_f have common matrices A and C, the left coprime factorization of each transfer matrix are given by

$$[\, G_u \; G_d \; G_f \,] = M^{-1} [\, N_u \; N_d \; N_f \,] \tag{8}$$

$$M = \left[\begin{array}{c|c} A + L_pC & L_p \\ \hline C & I \end{array}\right] \tag{9}$$

$$[\, N_u \; N_d \; N_f \,] =$$

$$\left[\begin{array}{c|ccc} A + L_pC & B_u + L_pD_u & B_d + L_pD_d & B_f + L_pD_f \\ \hline C & D_u & D_d & D_f \end{array}\right]. \tag{10}$$

where $A + L_pC$ is stable. Let consider a fault detection filter $H \in \mathbb{R}^{n_y\times n_y}$ for estimation error signal f_e as shown in Fig. 1. From equation (8), The estimation error signal f_e is given by

$$f_e = My - N_u u = N_d d + N_f f. \tag{11}$$

Therefore, the estimation error signal f_e depends on disturbance d and fault signal f. The following lemma is satisfied for the transfer matrix N_f.

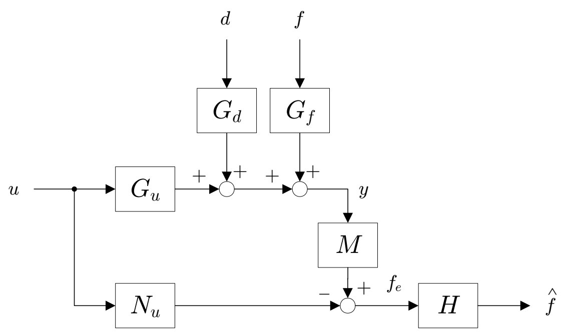

Fig. 1. Block Diagram of the Fault Detection Filter

***Lemma** 1.* (Zhou [1996]) Let the LTI system (5) be satisfied assumptions 1–3. Then the square and invertible transfer matrix $W_f \in \mathcal{R}H_\infty^{n_y\times n_y}$ exists such that

$$W_f W_f^* = N_f N_f^* \tag{12}$$

and W_f is given by

$$W_f = \left[\begin{array}{c|c} A + L_pC & (L_p - L_0)R_f^{\frac{1}{2}} \\ \hline C & R_f^{\frac{1}{2}} \end{array}\right] \tag{13}$$

where $R_f = D_f D_f^T$. and $L_0 := -(B_f D_f^T + YC^T)R_f^{-1}$ is obtained by the solution $Y \geq 0$ of following Ricatti equation.

$$\begin{aligned} &(A - B_f D_f^T R_f^{-1} C)Y + Y(A - B_f D_f^T R_f^{-1} C)^T \\ &-YC^T R_f^{-1} CY + B_f(I - D_f^T R_f^{-1} D_f)B_f^T = 0. \end{aligned} \tag{14}$$

where $A - B_f D_f^T R_f^{-1} C - YC^T R_f^{-1} C$ is stable.

Since the property of the singular value, $\sigma(W_f) = \sigma(N_f)$ and $\sigma(W_f^{-1} N_f) = 1$.

4. OPTIMIZATION PROBLEMS FOR FAULT DETECTION FILTER

From Fig. 1, the input/output relation of the filter H is given by

$$\hat{f} = Hf_e = HN_d d + HN_f f = G_{\hat{f}d} d + G_{\hat{f}f} f. \tag{15}$$

where $G_{\hat{f}d} := HN_d$ is a transfer matrix from disturbance d to filter output $\hat{f}$, and $G_{\hat{f}f} := HN_f$ is a transfer matrix from fault signal f to filter output $\hat{f}$. As mentioned above, the estimation signal f_e depends on not only fault signal, but also disturbance. So that the fault detection filter is required to have the performance for disturbance attenuation while the sensitivity for fault signal is maintained. In this paper, two optimization problems are formulated and the solution for each problem is obtained which method is based on the literature Liu [2007].

4.1 Filter A

We will show a problem for the fault detection filter.

Problem 1. Let an LTI system (5) be satisfied assumptions 1–3 and $\beta > 0$ be a given fault sensitivity level. Then find optimal fault detection filter $H \in \mathcal{R}H_\infty^{n_y \times n_y}$ such that $\|G_{\hat{f}d}\|_\infty$ is minimizing and $\|G_{\hat{f}f}\|_- \geq \beta$, i.e.

$$\min_{H \in \mathcal{R}H_\infty^{n_y \times n_y}} \Big\{ \|HN_d\|_\infty : \|HN_f\|_- \geq \beta \Big\}. \tag{16}$$

The optimal solution for Problem 1 is given by the following theorem.

***Theorem** 1.* (Filter A) Let an LTI system (5) be satisfied assumptions 1–3. Then the optimal solution for Problem 1 is given as follows.

$$H = \beta W_f^{-1} \tag{17}$$

***Proof** 1.* Let a fault detection filter H is represented as follows.

$$H = \Phi W_f^{-1}, \quad \Phi \in \mathcal{R}H_\infty^{n_y \times n_y} \tag{18}$$

Then, we have

$$\begin{aligned} \|HN_f\|_- &= \inf \underline{\sigma}(HN_f N_f^* H^*) \\ &= \inf \underline{\sigma}(HW_f W_f^* H^*) \\ &= \|HW_f\|_- \\ &= \|\Phi W_f^{-1} W_f\|_- \\ &= \|\Phi\|_- \geq \beta \end{aligned} \tag{19}$$

by the definition of the norm. On the other hand, following inequality is given.

$$\bar{\sigma}(HN_d) = \bar{\sigma}(\Phi W_f^{-1} N_d) \leq \bar{\sigma}(\Phi)\bar{\sigma}(W_f^{-1} N_d) \tag{20}$$

Therefore, $\|HN_d\|_\infty$ is minimizing with

$$\Phi = \beta \tag{21}$$

for minimizing $\bar{\sigma}(\Phi)$ which is represented in (19). Then, the optimal fault detection filter for Problem 1 is given by

$$H = \beta W_f^{-1}. \tag{22}$$

□

4.2 Filter B

We will show another problem for the fault detection filter.

Problem 2. Let an LTI system (5) be satisfied assumptions 1–3 and $\beta > 0$ be a given fault sensitivity level. Then find optimal fault detection filter $H \in \mathcal{R}H_\infty^{n_y \times n_y}$ such that $\|G_{\hat{f}d}\|_2$ is minimizing and $\|G_{\hat{f}f}\|_-^{[f_1,f_2]} \geq \beta$, i.e.

$$\min_{H \in \mathcal{R}H_2^{n_y \times n_y}} \Big\{ \|HN_d\|_2 : \|HN_f\|_-^{[f_1,f_2]} \geq \beta \Big\}. \tag{23}$$

Problem 2 is transformed as shown in the following theorem.

***Theorem** 2.* (Filter B) Let an LTI system (5) be satisfied assumptions 1–3. Now the fault detection filter H is formed

$$H = \Psi W_f^{-1}, \quad \Psi \in \mathcal{R}H_2^{n_y \times n_y} \tag{24}$$

then Problem 2 is transformed as follows.

Fig. 2. Magnetic Suspension System

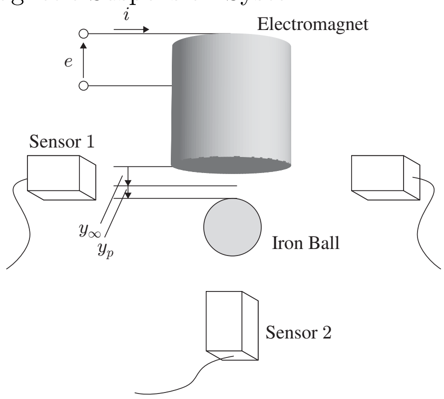

Fig. 3. Description of Magnetic Suspension System

Table 1. System Parameters

	Value
Mass M [kg]	0.357
Steady Gap y_∞ [m]	2.0×10^{-3}
Steady Current I [A]	0.397
Coefficient k [Nm^2/A^2]	9.370×10^{-5}
Position Offset Term y_0 [m]	4.490×10^{-3}
$K_y = \frac{2kI^2}{(y_\infty + y_0)^3}$	1.079×10^2
$K_i = \frac{2kI}{(y_\infty + y_0)^2}$	1.765

$$\min_{\Psi \in \mathcal{R}H_2^{n_y \times n_y}} \Big\{ \|\Psi W_f^{-1} N_d\|_2 : \|\Psi\|_-^{[f_1,f_2]} \geq \beta \Big\} \tag{25}$$

***Proof** 2.* Similarly in the proof of Theorem 1, following equation is satisfied from the definition of norm.

$$\|HN_f\|_-^{[f_1,f_2]} = \|\Psi\|_-^{[f_1,f_2]} \geq \beta \tag{26}$$

□

Filter B is calculated with a solution of the problem in Theorem 2 by using a optimization problem solver like simplex method.

5. FAULT DETECTION FILTER DESIGN

5.1 Model of the Plant

In this section, an 1-DOF magnetic suspension system as shown in Fig. 2 is modelled to design the fault detection filter and to structure a fault tolerant control system.

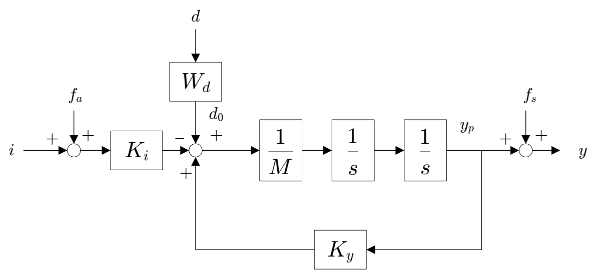

Fig. 4. Block Diagram of the Model

Description of the magnetic suspension system is shown in Fig. 3. where average value of two sensor information is utilized for feedback information.

5.2 State-Space Representation

We derive the equation of linearized motion of the iron ball as follows.

$$M\ddot{y}_p = K_y y_p - K_i i + d - K_i f_a \tag{27}$$

where d is the disturbance mainly perturbation of the mass, and f_a is the actuator fault signal. The output y is represented with the sensor fault signal f_s as follows.

$$y = y_p + f_s \tag{28}$$

Therefore, the state-space representation of whole system with pre weight function for the disturbance d is given by

$$\begin{cases} \dot{x} \;=\; Ax + B_u u + B_d d + B_f f \\ y \;=\; Cx + D_u u + D_d d + D_f f \end{cases} \tag{29}$$

$$A = \begin{bmatrix} 0 & 1 & 0 \\ \dfrac{K_y}{M} & 0 & \dfrac{1}{M}C_{d0} \\ 0 & 0 & A_{d0} \end{bmatrix}, B_u = \begin{bmatrix} 0 \\ -\dfrac{K_i}{M} \\ 0 \end{bmatrix} \tag{30}$$

$$B_d = \begin{bmatrix} 0 \\ \dfrac{1}{M}D_{d0} \\ B_{d0} \end{bmatrix}, B_f = \begin{bmatrix} 0 & 0 \\ -\dfrac{K_i}{M} & 0 \\ 0 & 0 \end{bmatrix} \tag{31}$$

$$C = [\,1\;\,0\;\,0\,]\,, D_u = 0, D_d = 0, D_f = [\,0\;\,1\,] \tag{32}$$

$$W_{d0} := \begin{cases} \dot{x}_{d0} \;=\; A_{d0}x_{d0} + B_{d0}d \\ d_0 \;=\; C_{d0}x_{d0} + D_{d0}d \end{cases}. \tag{33}$$

where $x = [y_p \; \dot{y}_p \; x_{d0}]^T$ and $f = [f_a \; f_s]^T$, and d_0 represents the disturbance. The pre weight function W_{d0} is chosen

$$W_{d0}(s) = 6.3096 \times 10^{-3} \cdot \frac{\frac{1}{2\pi \cdot 0.1}s + 1}{\frac{1}{2\pi \cdot 6}s + 1}. \tag{34}$$

The block diagram of the whole system is illustrated in Fig. 4.

5.3 Factorizations of the Model

To obtain the left coprime factorization of the model (29), the matrix L_p is decided with pole placement method. Let $\lambda_p = \{-100, \ -110, \ -260\}$ be the pole replaced, then the matrix $L_p = [-0.0043 \times 10^5 \ -0.4960 \times 10^5 \ 1.0189 \times 10^5]^T$. The frequency characteristics of the maximum singular value of N_d and the minimum singular value of N_f are shown in Fig. 5. Furthermore, the spectral factorized matrix W_f is obtained as follows.

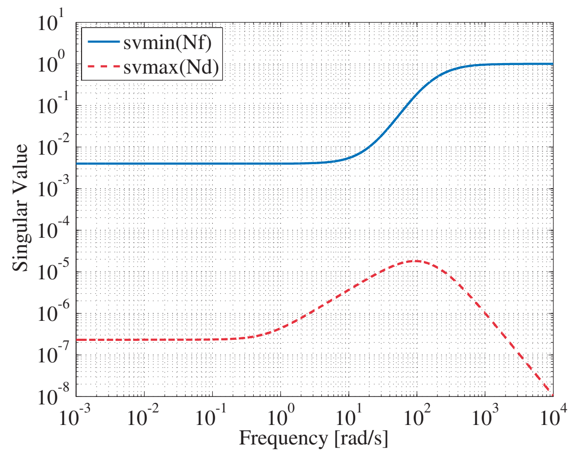

Fig. 5. The Singular Value of N_d and N_f

$$W_f = \left[\begin{array}{ccc|c} -432.3 & 1 & 0 & -397.5 \\ -4.93 \times 10^4 & 0 & -9.828 & -4.9 \times 10^4 \\ 1.019 \times 10^5 & 0 & -37.7 & 1.019 \times 10^5 \\ \hline 1 & 0 & 0 & 1 \end{array}\right] \tag{35}$$

5.4 Filter A for the Magnetic Suspension System

From Theorem 1, the optimal fault detection filter for Problem 1 is given by $H = \beta W_f^{-1}$. Let $\beta = 10$, the bode diagram of the filter is shown in Fig. 6 (a) by solid line. Moreover, characteristics of the singular value of $G_{\hat{f}d}$ and $G_{\hat{f}f}$ are shown in Fig. 5 (b). Because of the property, the singular value of N_f is uniformed by W_f^{-1}. In this case, $\|HN_f\|_- = 1.0$, $\|HN_d\|_\infty = 7.4424 \times 10^{-4}$.

5.5 Filter B for the Magnetic Suspension System

Let $[f_1, f_2] = [0.001, 8]$, $\beta = 100$ and dimension of Ψ be second. Then the optimal solution Ψ on Theorem 2 is given by

$$\Psi = \left[\begin{array}{cc|c} -3327 & 218.5 & -283 \\ -2578 & -418.3 & 1619 \\ \hline 81.57 & 28.92 & 0 \end{array}\right]. \tag{36}$$

In the process of above calculation, Genetic Algorithm and Melder-Mead Simplex Method are used to solve the problem shown in Theorem 2. As a result, Filter B which is an optimal solution for Problem 2 is consisted as $H = \Psi W_f^{-1}$. The bode diagram of Filter B is illustrated in Fig. 6 (a) by dotted line, and the characteristic of Ψ is shown in Fig. 6 (b). Furthermore, the frequency characteristics of the maximum singular value of $G_{\hat{f}d}$ and the minimum singular value of $G_{\hat{f}f}$ are affected as Fig. 6 (c). Then $\|HN_f\|_-^{[0.001,8]} = 100$ and $\|HN_d\|_2 = 0.231469$.

6. CONTROL SYSTEM DESIGN

In this section, controllers are designed to construct a fault tolerant control system based on GIMC structure.

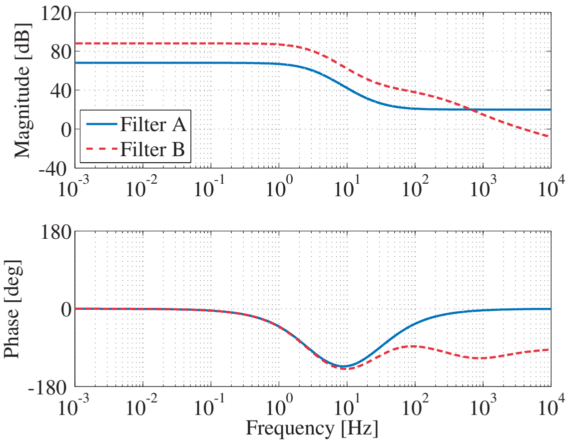

(a) Bode Diagram of the Filter A and B

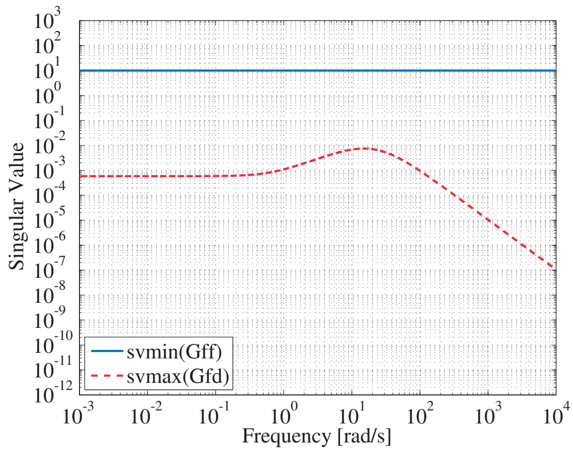

(b) The Singular Value of $G_{\hat{f}d}$ and $G_{\hat{f}f}$ with Filter A

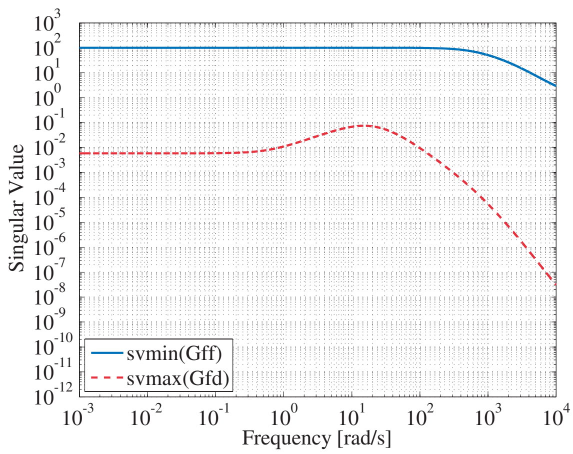

(c) The Singular Value of $G_{\hat{f}d}$ and $G_{\hat{f}f}$ with Filter B

Fig. 6. Characteristics of the Fault Detection Filter

6.1 Controller Design

The fault tolerant control system used in this paper is illustrated in Fig. 7. Where $\widetilde{P}$ represents the plant, U and V^{-1} the representation of left coprime factorization of K, Q the internal controller. The controller K is designed for the nominal plant. Furthermore, K is factorized to $K = V^{-1}U$ by the matrix L_k which is stabilizable $A_k + L_kC_k$. Similarly in the model, L_k is calculated by pole placement method.

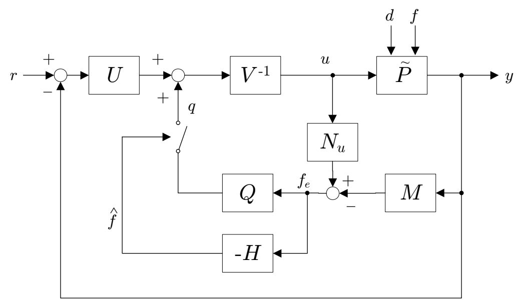

Fig. 7. Fault Tolerant Control System based on GIMC

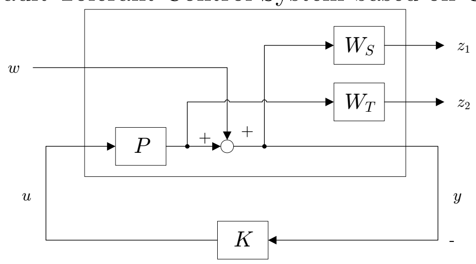

Fig. 8. Generalized Plant

6.2 Internal Controller Q

Internal Controller Q is given by $Q = V(K_Q - K)(N_uK_Q + M)^{-1}$, where the controller K_Q is designed to maintain stability for the plant occurred some faults. Since the degree of Q is high to implementation, however, 8 degrees system matrix Q_{bal} is obtained by balanced model reduction with evaluation of Hankel singular value.

7. EXPERIMENTAL RESULTS

In this section, experimental results are shown to evaluate designed fault detection filters. The scenario of the experiment is that the iron ball is suspended at the steady gap as the initial state, and the Sensor 1 is breaking down and the output keeps -2 [mm] after 1 [s]. It is a same case that the Sensor 2 is shut out completely.

Experimental results with Filter A and Filter B are shown in Fig. 9. Where the threshold $J_{th} = 0.011$ for Filter A, and $J_{th} = 0.12$ for Filter B. Sensors information time responses are shown in Fig. 9 (a). Since the average of values, Sensor 1 and Sensor 2 is feedbacked, it is controlled to be zero. After 1 [s], Sensor 2 is breaking down and output keeps -2 [mm]. Therefore, the equilibrium point is changed 2 [mm] to positive direction. From the results, filter output $\hat{f}$ is changed by occurring the sensor fault in both case, with filter A or filter B. The controller is reconfigured by the internal signal q when the filter output $\hat{f}$ over the threshold J_{th} i.e. the sensor fault is detected. Moreover, the stability is maintained by the reconfigured controller and the iron ball is suspended after the sensor fault occurred.

It is disturbance as the parameter perturbation that the mass of the iron ball is changed. The fault detection filter is expected to have properties, therefore, it has almost no effect from the disturbance, and it is separable between the disturbance and the fault signal. Similarly, the experimental results are shown in Fig. 10. The solid line represents the nominal case, the dotted line the result the case with -20% mass, and dashed line the result

Table 2. Convergence Value of $\hat{f}$

	Nominal case	$0.80 * M$	$1.21 * M$
Filter A	9.25×10^{-3}	-17.8 %	+62.7 %
FIlter B	7.26×10^{-2}	-0.08 %	+56.4 %

the case with +21% mass, respectively. It is ideal result that the filter output $\hat{f}$ does not depend on changing the mass of the iron ball, but both results are changed. Each convergence value and the fluctuation of the filter output $\hat{f}$ are summarized in Table 2. It is yielded about ±25% fluctuation when the sensor fault occurred with Filter A. In the case with Filter B, on the other hand, it can be attenuated less than ±10% effect from the disturbance. It can be improved to consider the specific frequency range for the norm for Filter B compared with Filter A.

8. CONCLUSIONS

In this paper, two optimization problems were formulated for the fault detection filter, and the optimal solutions were introduced respectively. The magnetic suspension system was modelled as an LTI system including disturbance and fault signals and fault detection filters were designed for this system. Furthermore, controllers were designed for the nominal plant and the faulty plant respectively to construct the GIMC structure. It was verified that designed fault detection filters were valid for the fault tolerant control system experimentally. Finally, designed fault detection filters were compared and it was shown that Filter B has better performance for disturbance attenuation.

REFERENCES

K. Zhou and Z. Ren, "A New Controller Architecture for High Performance, Robust, and Fault-Tolerant Control," *IEEE Trans. on Automatic Control*, vol. 46, no. 10, 2001.

K. Zhou, "A Natural Approach to High Performance Robust Control: Another Look at Youla Parameterization," *Proc. in SICE Annual Conference*, pp. 869-874, 2004.

T. Namerikawa and H. Maruyama, "High Performance Robust Control of Magnetic Suspension Systems Using GIMC Structure," *Trans. on the Society of Instrument and Control Engineers*, vol. 42, no.11, pp. 1181-1187, 2006.

R. J. Patton, "Fault-Tolerant Control Systems: The 1997 Situation," *Proc. in IFAC Safeprocess Conference*, pp. 1033-1054, 1997.

Y. Zhang and J. Jiang, "Bibliographical Review on Reconfigurable Fault-Tolerant Control Systems," *Proc. in IFAC Safeprocess Conference*, pp. 265-276, 2003.

D. U. Campos-Delgado and K. Zhou, "Reconfigurable Fault-Tolerant Control Using GIMC Structure," *IEEE Trans. on Automatic Control*, vol. 48, no. 5, 2003.

H. Niemann, "Fault Tolerant Control based on Active Fault Diagnosis," *Proc. in American Control Conference*, pp. 2224-2229, 2005.

N. Liu and K. Zhou, "Optimal Solutions to Multi-objective Robust Fault Detection Problems," *IEEE Conference on Decision and Control*, pp. 981-988, 2007.

K. Zhou and J. C. Doyle, *Robust and Optimal Control*, Prentice Hall, 1996.

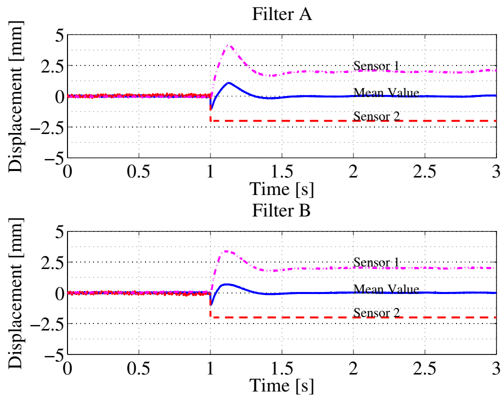

(a) Time Response of the Gap y_p

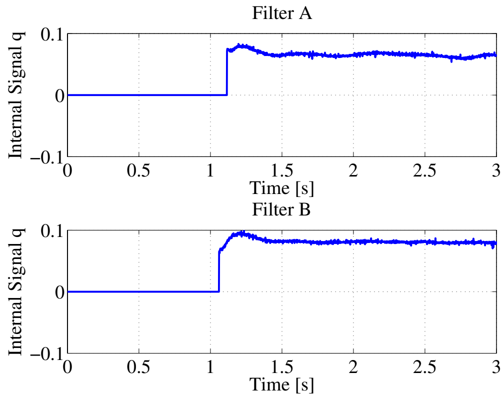

(b) Time Response of the Internal Signal q

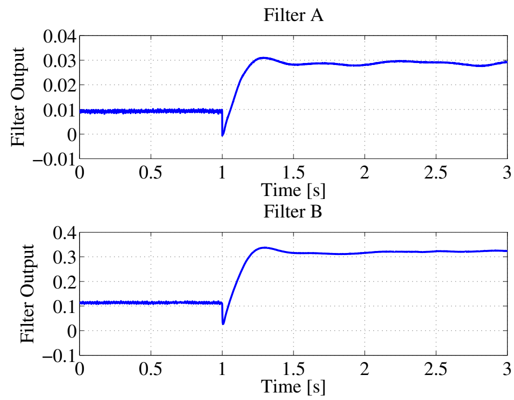

(c) Time Response of the Filter Output $\hat{f}$

Fig. 9. Experimental Results

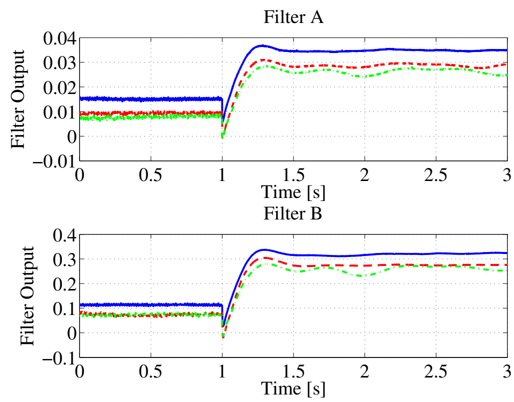

Fig. 10. Influence of Perturbed Mass to $\hat{f}$